#### Refrigeration

#### Manuscript Draft

Manuscript Number: JIJR-D-16-00625

Title: Availability and Exergy Analysis of Electrically- and Thermally-driven Engines to Drive Heat Pumps: An Exhaustive Comparative Study

Article Type: Research Paper

Keywords: heat pumps, ground-source, sorption, thermodynamics

Abstract: The choice of driving a heat pump with an electrically- or a thermally-driven engine is a vexing question complicated by the carbon footprint and environmental impact of using electricity versus natural gas (or waste heat) as the main driver for the respective engines. Useful work generated by these two distinct engines is the focal point of this paper, addressing a key question: which engine presents a better choice for a given heat pumping application within the constraints of energy and environmental stewardship?

We examine this question comprehensively through the methodology of energy, exergy, and availability analysis, explaining clearly, why the output of work from these two distinct engines is inherently vastly different. Thermodynamic consistency is guaranteed by satisfaction of the First and Second Laws applied to closed systems and their subsystems. The general conclusion is that thermally-driven engines are not industrious converters of heat to mechanical work.

## **Highlights (for review)**

## Highlights

- Features of the electrically- and thermally-driven heat engines used to drive heat pumps for refrigeration and space conditioning applications
- Which engine may be a better choice for a given application
- Detailed energy and exergy analysis to support the conclusions
- Extensive cross checks of the results from analysis

# Availability and Exergy Analysis of Electrically- and Thermally-driven Engines to Drive Heat Pumps: An Exhaustive Comparative Study<sup>☆</sup>

Moonis R. Ally<sup>1</sup>, Vishaldeep Sharma, Omar Abdelaziz

 $Energy\ and\ Transportation\ Sciences\ Division,\ Oak\ Ridge\ National\ Laboratory,\ Oak\ Ridge,$   $Tennessee\ 37831$ 

#### Abstract

The choice of driving a heat pump with an electrically- or a thermally-driven engine is a vexing question complicated by the carbon footprint and environmental impact of using electricity versus natural gas (or waste heat) as the main driver for the respective engines. Useful work generated by these two distinct engines is the focal point of this paper, addressing a key question: which engine presents a better choice for a given heat pumping application within the constraints of energy and environmental stewardship? We examine this question comprehensively through the methodology of energy, exergy, and availability analysis, explaining clearly, why the output of work from these two distinct engines is inherently vastly different. Thermodynamic consistency is guaranteed by satisfaction of the First and Second Laws applied to closed systems and their subsystems. The general conclusion is that thermally-driven engines are not industrious converters of heat to mechanical work.

Keywords: heat pumps, ground-source, sorption, thermodynamics,

<sup>&</sup>lt;sup>☆</sup>This manuscript has been authored by UT-Battelle, LLC under Contract No. DE-AC05-00OR22725 with the U.S. Department of Energy. The United States Government retains and the publisher, by accepting the article for publication, acknowledges that the United States Government retains a non-exclusive, paid-up, irrevocable, world-wide license to publish or reproduce the published form of this manuscript, or allow others to do so, for United States Government purposes. The Department of Energy will provide public access to these results of federally sponsored research in accordance with the DOE Public Access Plan (http://energy.gov/downloads/doe-public-access-plan).

<sup>&</sup>lt;sup>1</sup>Corresponding author. E-mail: allymr@ornl.gov; Ph:(865)-576-8003; Fax:(865)-574-9338

#### sustainability

2010 MSC: 00-01, 99-00

#### Nomenclature

#### Acronyms

- $\dot{A}$  rate of availability, kW
- $\dot{I}$  thermodynamic rate of Irreversibility,  $T_o \dot{\sigma}$ , kW
- $\dot{m}$  mass flow rate,  $kg \cdot s^{-1}$
- $\dot{Q}$  rate of thermal energy, kW
- $\dot{W}$  rate of work, kW
- AHP Absorption Heat Pump
- COP Coefficient of Performance
- E energy, kJ
- EES Engineering Equation Solver
- q gravitational acceleration,  $m \cdot s^{-2}$
- GHG Greenhouse gases
- GWP Greenhouse Warming Potential
- h specific enthalpy,  $kJ \cdot kg^{-1}$
- HFO Hydrofluoro-olefin
- P pressure, bar
- $R \qquad \text{universal gas constant, } kJ \cdot kg^{-1} \cdot K^{-1}$
- S entropy,  $kJ \cdot K^{-1}$

- s specific entropy,  $kJ \cdot kg^{-1 \cdot K^{-1}}$
- T temperature,  ${}^{o}C$  or
- t Time, s
- U internal energy, kJ
- u specific internal energy,  $kJ \cdot kg^{-1}$
- V velocity,  $m \cdot s^{-1}$



z elevation above a datum level, m

#### **Greek Symbols**

- $\dot{\sigma}$  rate of entropy generation,  $kW \cdot K^{-1}$
- $\eta$  compressor or pump efficiency, dimensionless

#### Subscripts

- a actual
- cv control volume
- j th thermal reservoir, or component
- abs absorber
- boiler boiler in the distillation column
- c condenser, or cooling
- e evaporator
- h heating
- min minimum
- o reference state

#### 1. Introduction

Commercial and residential heat pumps are predominantly run using electricallydriven engines (compressors) due to their reliability, compactness, low maintenance, and favorable cost. In contrast, thermally-driven heat pumps—operating on sorption effects—are inherently physically large, with lower coefficient of performance based on site energy use, than their electrical counterparts. Renewed interest is shown in thermally-driven heat pumps because they are essentially independent of, or supportive of, the electrical grid. In addition, thermallydriven heat pumps use refrigerants that have zero Greenhouse Warming Potential (GWP), which is in sharp contrast to the electrically-driven heat pumps that mainly work with high-GWP refrigerants—with two exceptions: carbon dioxide (R-744) and ammonia (R-717) and newer HFO blends and hydrocarbons [1], [2]. The idea that thermally-driven systems are, on the whole, more environmentally friendly than vapor compression heat pumps seems appealing, especially if the electricity driving the vapor compression heat pumps is derived from burning coal. Absorption (a subset of sorption) is receiving increased attention as an enabling technology to utilize fuel more effectively, reduce pollution, and to serve multiple thermal loads simultaneously. For example, integration of absorption with micro gas turbines uses a wide range of fuels to simultaneously produce electricity, cooling, and heating (so called combined cooling, heating, and power, or CCHP systems) [3, 4]. Other applications include fuel-driven Absorbtion Heat Pump (AHP) water heating [5, 6, 7], compression absorption heat pump for large temperature  $(90^{\circ}C)$  lifts [8, 9], solar-assisted absorption heat pumps [10, 11, 12, 13, 14], district heating [15, 16, 13, 17], and thermal energy storage [18, 19]. Many examples of industrial applications of absorption heat pumps can be found in drying [20, 21, 22], distillation [23, 24, 25, 26], and evaporation [27, 28]. The predominant working pairs in absorption technology are LiBr-H<sub>2</sub>O, NH<sub>3</sub>-H<sub>2</sub>O, and to a limited extent, NaOH-H<sub>2</sub>O with few exceptions [20].

Since natural gas emits approximately half the carbon dioxide as conven-

tional coal plants to produce electricity [29], it is viewed as an acceptable "bridge" fuel to cut greenhouse gas (GHG) emissions. The target submitted by the United States to the United Nations Framework Convention on Climate Change (UNFCCC) is to reduce GHG emissions by 26–28% below 2005 levels by 2025, and to make best efforts to reduce it by 28% [30]. The growing supply of natural gas in the United States may serve as an interim stopgap surrogate for aging coal-fired power plants, but it is not an answer to the problem of accumulating atmospheric  $CO_2$  levels, which have reached 404.48 ppm as of June 2016 [31]—up from 286 ppm at the start of the industrial revolution, circa 1781, the year James Watt patented the Steam Engine. For the year to date (June 2016), the average global temperature was  $1.05^{\circ}C$  above the 20th century average, surpassing the previous record for this period set in 2015 by 0.20°C. Scientists of the American Geophysical Union (AGU) agree that the detailed temperature record of the 20th century cannot be explained without bringing to bear human effects and GHG emissions [32]. How long natural gas shall serve as a bridge fuel to generate electricity is debatable. Since heat pumps are indispensable in reducing the demand on primary energy resouces by harnessing renewable or waste energy and converting it to a useful utility, it is incumbent to provide the most appropriate choice of engines to drive them.

This paper discusses the question of whether an electrically-driven engine or a thermally-driven engine is a more efficient consumer of the source energy. The methodology relies on energy, exergy, and availability analysis to quantify mechanical work produced by the engines, entropy production, and process Irreversibility, the true measure of thermodynamic "Lost Work."

An ammonia vapor compression heat pump is considered first, followed by the thermally-driven ammonia-water absorption heat pump. Design features such as heat transfer coefficients in heat exchangers, wettability, approach temperatures, distillation and rectification plate spacings, superficial velocity, flooding, and other technical issues important to the design engineer are eschewed,

because these details are unnecessary for the type of analysis required to address the question of interest. The analyses' calculation basis is to provide 175.6 kW

( $\approx 50$  tons) of refrigeration at an evaporator temperature of 0  $^{o}C$  and to reject heat at 50  $^{o}C$  in the condenser. These temperatures are chosen because they fall within close proximity to acceptable ranges of refrigeration, space conditioning, and water heating applications. Ammonia is suitably the refrigerant of choice since it is used in vapor compression, and in absorption machines.

#### 2. Methodology

The methodology consists of applying energy balances, entropy generation, and availability analysis to the electrically- and thermally-driven heat pumps to quantify the mechanical work produced by these two different engines to drive the heat pump.

The energy balance from the First Law of thermodynamics is expressed by Equation (1)[33]:

$$\sum \dot{Q}_{cv} + \dot{W}_{cv} + \sum_{in} \dot{m} \left( h + \frac{V^2}{2} + gz \right) - \sum_{out} \dot{m} \left( h + \frac{V^2}{2} + gz \right)$$

$$= \frac{dE_{cv}}{dt} = \frac{d}{dt} \left[ m \left( u + \frac{V^2}{2} + gz \right) \right]$$
(1)

where  $\dot{Q}_{cv}$  and  $\dot{W}_{cv}$  represent the rate of thermal energy and work, respectively, supplied to the control volume (cv);  $\dot{m}$  is the mass flow rate in and out of the control volume;  $h, \frac{V^2}{2}$ , and gz represent the enthalpy, kinetic, and potential energy terms of the mass flow; and u is the internal energy per unit mass of the fluid flowing in the control volume. The term  $\frac{dE_{cv}}{dt}$  is the rate of accumulation of energy within the control volume, where  $E_{cv} = m\left(u + \frac{V^2}{2} + gz\right)$ . Note that both  $\dot{Q}_{cv}$  and  $\dot{W}_{cv}$  are defined as positive when they are inputs to the control volume.

The general entropy production equation is

$$\frac{dS_{cv}}{dt} + \sum_{out} \dot{m}(s) - \sum_{in} \dot{m}(s) = \sum_{in} \frac{\dot{Q}}{T} + \dot{\sigma_{cv}}.$$
 (2)

Since the First Law Equation (1) contains work terms but no entropy terms, and the Second Law Equation (2) contains entropy terms but no work terms, it

is useful to combine the two to yield:

$$\dot{W}_{cv} = \sum_{out} \dot{m} \left( h - T_o s + \frac{V^2}{2} + gz \right) - \sum_{in} \dot{m} \left( h - T_o s + \frac{V^2}{2} + gz \right),$$

$$- \sum_{out} \dot{\sigma}_j \left( 1 - \frac{T_o}{T_j} \right) + \frac{dE_{cv}}{dt} - T_o \left[ \frac{dS_{cv}}{dt} - \dot{\sigma}_{total} \right]$$
(3)

where  $T_o$  is the reference temperature taken to be 273.15 K;  $\dot{Q}_j$  is the heat transfer at the control surface to or from thermal reservoirs at  $T_o$  or  $T_j$ ;  $S_{cv}$  is the entropy within the control volume; and  $\dot{\sigma}_{cv}$  is the total rate of entropy generation. Under steady-state conditions, Equation (1) is reduced to

$$\sum \dot{Q}_{cv} + \dot{W}_{cv} + \sum_{in} \dot{m} \left( h + \frac{V^2}{2} + gz \right) - \sum_{out} \dot{m} \left( h + \frac{V^2}{2} + gz \right) = 0, \quad (4)$$

and under steady-state and no-flow conditions, Equations 2 and 3 reduce to

$$\dot{\sigma}_{cv} = -\sum \frac{\dot{Q}_j}{T_j} \tag{5}$$

and

$$\dot{W}_{cv,actual} = -\sum \dot{Q}_j \left( 1 - \frac{T_o}{T_i} \right) T_o \dot{\sigma}_{cv}, \tag{6}$$

with  $\dot{I}_{cv} = T_o \dot{\sigma}_{cv}$ .

The minimum steady-state, no-flow rate of work,  $W_{cv}$  is when the entropy generation term is zero:

$$\dot{W}_{cv,min} = -\sum \dot{Q}_j \left( \frac{T_o}{T_j} \right). \tag{7}$$

The International Union of Pure and Applied Chemistry (IUPAC) convention, used in this paper, defines the change in internal energy as  $\Delta U_{cv} = \sum Q_{cv} + W_{cv}$  [34]. Throughout this paper, the useful work produced by the electrically-driven engine or the thermally-driven engine shall be calculated from the equation for the First Law, followed by an availability analysis, and the combined form of the First and Second Laws depicted by Equation (3). The First Law has a work term, but no entropy terms. The Second Law has entropy terms but no work term. Their combined form ([33]), described by Equation (3), reveals systemic Irreversibility vital to explaining the characteristic differences between the two engines—the focus of this paper.

#### 3. Electrically-Driven Vapor Compression Heat Pump

#### 3.1. First Law Analysis of the Electrically-Driven Heat Pump

A standard vapor compression heat pump (Figure 1) operating on the basis stated in the introduction is modeled using the Engineering Equation Solver (EES) software [35]. The corresponding p-h and T-s diagrams shown in Figure 2 and Figure 3, respectively, display relevant properties at the state points around the heat pump cycle. The compression efficiency, taken as 0.7, is representative of current technology. The expansion valve (EXV) is customarily treated as isenthalpic but has a large entropy change across it (Figure 3). The engine section consists of the electrically-driven adiabatic<sup>1</sup> compressor; and the heat pump section consists of the condenser, evaporator, and the EXV. The state properties for three cases of compressor efficiencies,  $0.7 \le \eta \le 1.0$ , are summarized in Table 1. Ignoring kinetic energy, potential energy, pressure drop, and heat loss from the compressor casing—on the basis that it is small compared to the work output [38], [36] and unimportant to the central theme of this paper the energy balance for the cycle-through application of Equation (1) and the state properties computed from the EES model are summarized in Table 1. A straightforward application of the First Law for the  $\eta = 0.7$  case yields the compressor work to the heat pump as positive (56.69 kW); when added to the thermal heat input (175.7 kW) to the evaporator, it equals the heat rejected via the condenser (-232.4 kW). Similarly, for the other two cases when  $\eta = 0.9$ and  $\eta = 1.0$  the energy balance equation is fully satisfied for the control volume around the heat pump as summarized in Table 2. As compressor efficiency

<sup>&</sup>lt;sup>1</sup>The assumption of an adiabatic compressor is more of a convenience than a necessity. For details on compressor heat losses, see [36], [37]

increases, the work required to drive the heat pump and the heat rejected via the condenser both decrease for the same refrigeration load. The variation in condenser load in going from a compressor efficiency of 1 to 0.7 is not significant <sup>2</sup>. Our primary focus is on the useful work produced by the electrically-driven engine needed to drive the heat pump portion of the cycle.

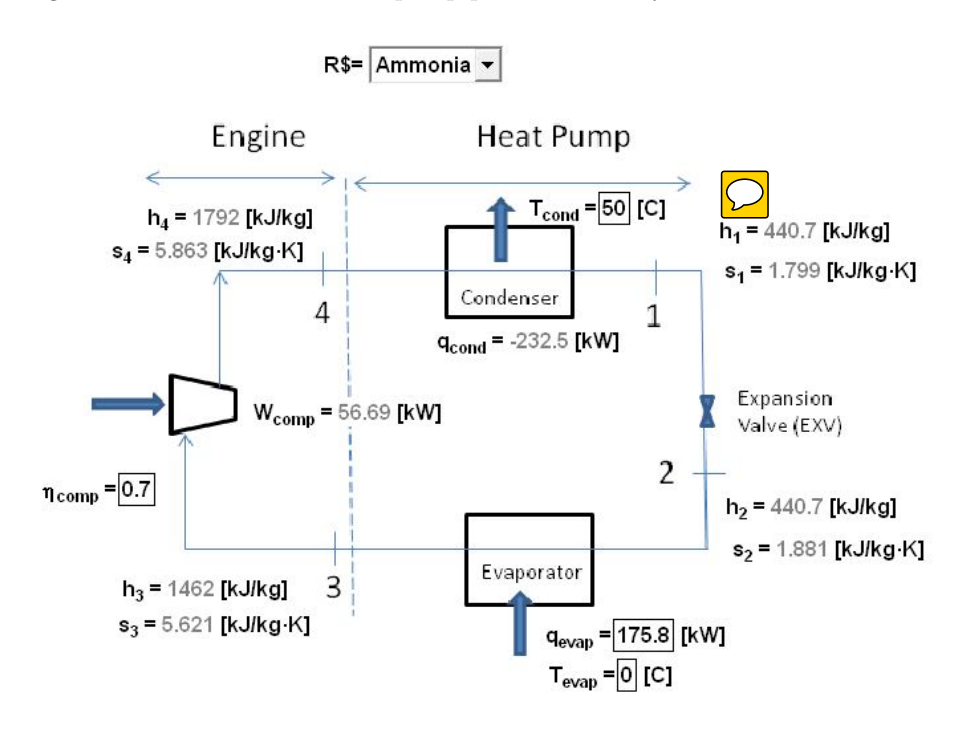


Figure 1: A standard vapor compression heat pump demarcated into Engine and Heat Pump sections. The refrigerant is ammonia.

 $<sup>\</sup>overline{\phantom{a}^2}$  Typical compressor efficiencies are 70% -85% [39]. Higher efficiency bounds the achievable limits.

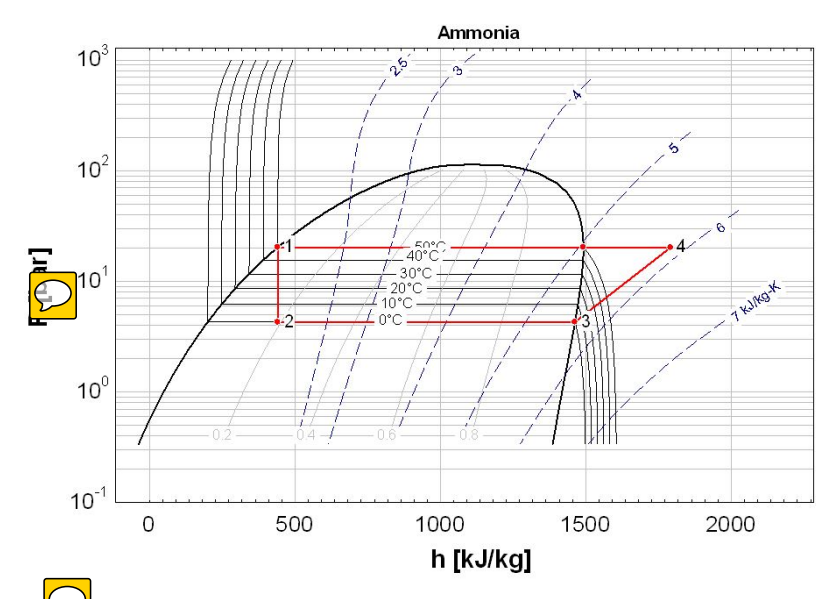


Figure 2. Pressure enthalpy at state points from the simulation of the vapor compression cycle of Figure 1 using EES.

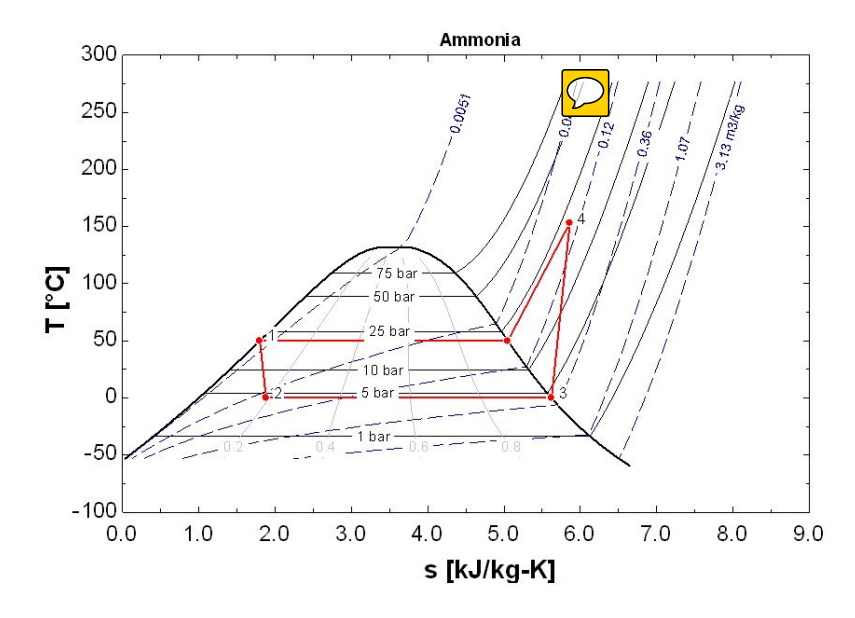


Figure 3: Temperature entropy at state points from the simulation of the vapor compression cycle of Figure 1 using EES.

Table 1: State points from simulation in EES for compressor efficiencies designated by  $\eta$ ;  $T_{e} = 0$   $^{o}C$ ; and  $T_{o} = 25$   $^{o}C$ 

$\eta = 0.7$									
State Point	Т	F C	h	s	Quality	$\dot{m}$			
	$(^{o}C)$	(bar)	$kJ \cdot kg^{-1}$	$kJ \cdot kg^{-1} \cdot K^{-1}$		$kg \cdot s^{-1}$			
1	50	20.33	440.7	1.799	0	0.172			
2	0	4.296	440.7	1.881	0.1908	0.172			
3	0	4.296	1462	5.621	1	0.172			
4	153.4	20.33	1792	5.683	1	0.172			
			$\eta = 0$	0.9					
1	50	20.33	440.7	1.799	0	0.172			
2	0	4.296	440.7	1.881	0.1908	0.172			
3	0	4.296	1462	5.621	1	0.172			
4	125.5	20.33	1718	5.686	1	0.172			
$\eta=1.0$									
1	50	20.33	440.7	1.799	0	0.172			
2	0	4.296	440.7	1.881	0.1908	0.172			
3	0	4.296	1462	5.621	1	0.172			
4	116	20.33	1693	5.621	1	0.172			

Table 2: Energy balance for components in the simple electrically-driven heat pump cycle calculated from EES (compressor  $\eta=0.7,\,\eta=0.9,$  and  $\eta=1.0$ );  $T_c=50~^oC;\,T_e=0~^oC;$  and  $T_o=25~^oC$ 



$\eta = 0.7$								
Component	Energy In	Energy Out						
	kW	kW						
Actual work produced, $\dot{W}_{actual,VC}$	+56.69							
Evaporator	175.6							
Condenser		-232.4						
Total	232.3	-232.4						
$\eta = 0.9$								
Actual work produced, $\dot{W}_{actual,VC}$	+44.03							
Evaporator	175.6							
Condenser		-219.7						
Total	219.6	-219.7						
$\eta = 1.0$								
Actual work produced, $\dot{W}_{actual,VC}$	+39.73							
Evaporator	175.6							
Condenser		-215.4						
Total	215.3	-215.4						



## 3.2. Availability Analysis: Generic Non-Flow Configuration of the Electricallydriven Heat Pump

Another way of calculating the mechanical work required to drive the heat pump of Figure 1 is by using a more generic representation of the cycle to which availability analysis is applied. Such a representation does not need any specification of the nature of the refrigerant, fluid flow rates, or the engine type as it would in the EES model. For the same conditions of thermal loads and temperatures, the required work is obtained by applying Equation (6) to various components. Our focus is to determine the work supplied by the engine to drive the heat pump and to show consistency with the results calculated from the First Law, as summarized in Table 2. An added benefit of using availability analysis is that it reveals systemic inefficiencies which the First Law alone cannot reveal.

We apply Equation (6) to the evaporator in two parts. The first part consists of the first term on the right hand side of the equation, and the second part consists of evaluating  $T_o\dot{\sigma}_e$ . This is done to show the relative magnitudes of work and Irreversibility. The evaporator availability is given by Equation (8):

$$\dot{A}_{e,VC} = \dot{Q}_e \left( 1 - \frac{T_o}{T_e} \right). \tag{8}$$

Since  $T_o > T_e$  and  $\dot{Q}_e$  is > 0 (by convention),  $\dot{A}_{e,VC} =$  -16.08 kW.

Applying Equation (5) yields the entropy generation,  $\dot{\sigma}_e = \frac{\dot{Q}_e}{T_e}$  (0.6431  $K^{-1}$ ). The evaporator Irreversibility—the second term on the right in Equation (6)—is then given by the product  $T_o \dot{\sigma}_e$ .

Similarly, noting that  $\dot{Q}_c < 0$  (by convention); the condenser availability,  $\dot{A}_{c,VC} = \dot{Q}_c \left(1 - \frac{T_o}{T_c}\right)$  7.98  $kW \cdot K^{-1}$ ); entropy generation,  $\dot{\sigma}_c = 17.98$   $kW \cdot K^{-1}$ ); and Irreversibility,  $T_o \dot{\sigma}_c (-0.7192 \text{ kW})$ , are readily calculated.

The minimum work to drive the heat pump calculated from Equation (7) is 34.06 kW. Summing the entropy generation rates of the evaporator and condenser and then applying Equation (5) yields  $\dot{\sigma}_{cv} = 0.076 \ kW \cdot K^{-1}$ . The total heat pump Irreversibility is the product of  $T_o$  and  $\dot{\sigma}_{cv}$  70 kW).

The actual work necessary is the sum of the minimum work and the total

cycle Irreversibility (Lost Work)—whose sum is 56.76 kW— in good agreement with the First Law (56.69 kW) using EES simulation, thereby verifying our methodology and calculation procedures.

The results of the availability calculations for compressor efficiencies  $0.7 \le \eta \le 1.0$  are tabulated in Table 3.

Agreement between the actual compressor work ( $\dot{W}_{actual,VC}$ ) determined from the First Law analysis matches the availability analysis exceedingly well, as shown by comparing values in Tables 2 and 3. The total cycle Irreversibility is the highest (27.70 kW) when the compressor is least efficient ( $\eta = 0.7$ ), and it is the lowest (6.99 kw) when the compressor efficiency is at its maximum value ( $\eta = 1$ ). Similarly, the actual work required to drive the heat pump varies from 56.76 kW to 39.73 kW as  $0.7 \le \eta \le 1$ .

# 3.3. Second Law Analysis: Flow Configuration of the Electrically-Driven Heat Pump

For a comprehensive analysis, we resort to applying Equation (2) to the system shown in Figure 1 to prove that the actual work required by the electrically-driven engine is in agreement with our previous two calculations for each of the three cases of compressor efficiencies,  $\eta = 0.7$ , 0.9, and 1.0.

Under the assumption of steady-state and neglecting kinetic and potential energy terms, Equation (3) reduces to Equation (9).

$$\dot{W}_{cv} = \sum_{out} \dot{m} \left( h - T_o \right) - \sum_{in} \dot{m} \left( h - T_o \right) - \sum_{in} \dot{\sigma}_j \left( 1 - \frac{T_o}{T_j} \right) + T_o \dot{\sigma}_{total}. \tag{9}$$

The state points derived from the EES simulations used for Equation (3) are from Table 1. Its application to the three cases of compressor efficiency  $(\eta)$  further quantifies component-wise and systemic Irreversibility and reaffirms the work of the electrically-driven engine required to drive the heat pump by the previous two methods.

As compressor efficiency increases, its entropy generation rate  $(\dot{\sigma})$  decreases, becoming zero when  $\eta = 1$ . Since the compressor does not need to overcome

Table 3: Minimum and actual work supplied by the electrically-driven engine to drive the generic heat pump at various compressor efficiencies

	$\dot{I}_{VC} = T_o \dot{\sigma}_{VC}$ $\dot{W}_{actual,VC} = \dot{W}_{min,VC} + \dot{I}_{VC}$	(kW)	56.76		44.03		39.73
	$\dot{I}_{VC} = T_o \dot{\sigma}_{VC}$	(kW)	22.70		10.96		6.99
	$\dot{\sigma}_{VC} = -\sum \left(rac{Q_j}{T_j} ight)$	Ş			0.037		0.023
	$\sum rac{\dot{Q}e}{T_e}$	5	0 433		0.6431		0.6431
$\eta = 0.7$	$\sum \frac{\dot{Q}_c}{T_c}$ $\sum \frac{\dot{Q}_e}{T_e}$		(L) (V)	ا ا	-0.6799 0.6431	$\eta = 1.0$	-0.6665 0.6431
	$\dot{W}_{min,VC} = -\sum_{r} \dot{Q} \left(1 - \frac{T_o}{T_j}\right)$	(k)	34.06		33.07		32.74
	$\dot{A}_{c,VC} = \dot{Q}_c \left( 1 - \frac{T_o}{T_c} \right)$	(kW)	-17.98		-17.00		-16.66
	$\dot{A}_{e,VC} = \dot{Q}_e \left( 1 - \frac{T_o}{T_e} \right)$	(kW)	-16.08		-16.08		-16.08

Table 4: Entropy generation, Irreversibility, and performance metrics for the vapor compression cycle with  $T_c = 50 \text{ }^oC$ ;  $T_e = 25 \text{ }^oC$ ; and  $0.7 \le \eta \le 1.0; \ \dot{m} = 0.172 kg \cdot s^{-1}$ 

$\sum_{out}\dot{m}\left(h-T_os ight)$	$\sum_{out} \dot{m} \left( h - T_o s \right) \left  \sum_{in} \dot{m} \left( h - T_o s \right) \left  \sum_{j} \dot{Q}_{j} \left( 1 - \frac{T_o}{T_j} \right) \right $		ر.	İdronp.	$ \dot{W}_{actual,VC} $
(kW)	(kW)	(kW)		(kW)	(kW)
		$\eta = 0.7$			
7.558807	-36.791	$0 \approx$	12.4102	$12.4102 \mid 0.041624 \mid$	56.76
		$\eta = 0.9$			
3.90768	-36.791	0 ≈	0.01118	0.01118 3.3333	44.03
		$\eta = 0.9$			
2.9410	-36.791	0 ≈	0	0	39.73

as much "Lost Work" at higher levels of  $\eta$  as it does at lower levels, the total work required to drive the heat pump decreases as  $\eta$  increases. The work produced by the electrically-driven engine to drive the heat pump from the Second Law analysis (Table 4) precisely matches the values obtained by the First Law analysis (Table 2) and the availability analysis (Table 3), thereby completely validating our analysis.

We have yet to show that the total Irreversibility of the electrically-driven engine—combined with the heat pump cycle from the Second Law analysis for the flow system—agrees with the values calculated from the availability analysis ( $\dot{I}_{VC}$  in Table 3). To accomplish this, we utilize the properties from Table 1 to calculate  $\dot{\sigma}$  from Equation (2) to determine the Irreversibility for each component; we then add them up for the entire cycle as shown in Table 5. We see precise agreement between  $\dot{I}_{VC}$  and the total Irreversibility ( $\dot{I} = T_o \dot{\sigma}$ ) calculated by the two different methods mentioned above.

#### 3.4. Performance Metrics and Source Energy Consumption

The heating and cooling coefficient of performance and the source energy consumption are tabulated in Table 6 based on the evaporator, condenser, and compressor workloads shown in Table 2. The efficiency of a power plant that converts a fuel into heat and subsequently into electricity is measured by the heat rate: the amount of energy used by the power plant to generate one kilowatthour (kWh) of electricity. The inverse of the heat rate is the power plant efficiency, which for coal- and gas-fired plants is typically 33–45%, respectively [40]. We adopt 33% rather than 45 our analysis because it provides a more conservative (higher) figure for the source party consumption.

Table 5: Energy generation and Irreversibility for each component in the electrically-driven heat pump cycle with  $T_c=50$  °C;  $T_e=0$  °C;  $T_o$  °C; and  $0.7 \le \eta \le 1.0$ ; with  $\dot{m}=0.172kg\cdot s^{-1}$ 

$\eta = 0.7$						
$\dot{\sigma}_{VC}$	$\dot{I} = T_o \dot{\sigma}$					
$kW \cdot K^{-1}$	kW					
0.041624	12.41					
0.0202	6.03					
0.0141	4.21					
0.000177	0.053					
0.0761	22.70					
$\eta = 0.9$						
0.01118	3.3333					
0.0113	3.371					
0.0141	4.21					
0.000177	0.053					
0.03676	10.96					
$\eta = 1.0$						
0	0					
0.0092	2.73					
0.0141	4.21					
0.000177	0.053					
0.02348	6.99					

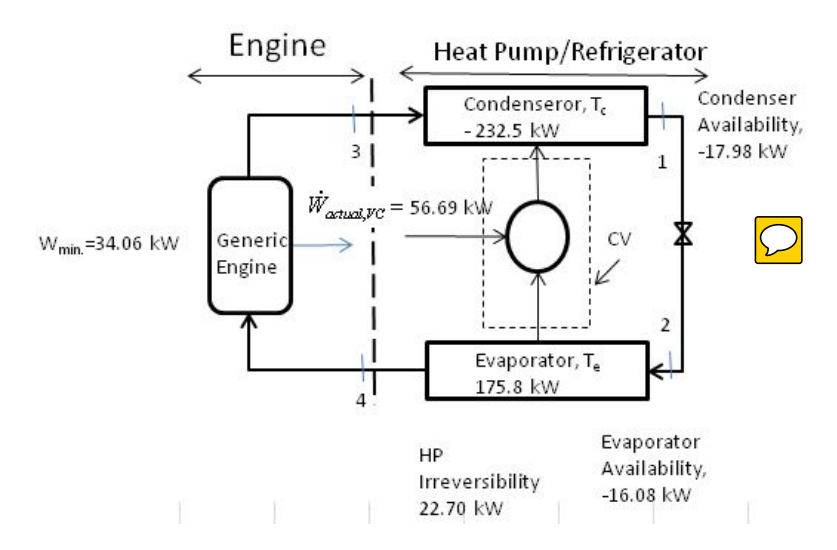


Figure 4: The generic representation of the engine and heat pump configuration of Figure 1.

The work supplied by an electrically-driven engine, used to drive the heat pump shown in Figure 4 for the lowest value of the compressor efficiency considered in this study ( $\eta = 0.7$ ), is  $\dot{W} = -56.76$  kW, consuming 172 kW at the source. Higher compressor efficiencies consume less energy at the source as shown in Table 6. The First Law provides information on the work and thermal loads, but the Second Law is necessary to provide information on how systemic inefficiency is distributed. The most inefficient components depend on the compressor efficiency as shown in Table 5. When  $\eta = 0.7$ , the order of Irreversibility is compressor > condenser > EXV > evaporator. However, this Irreversibility hierarchy changes to EXV > condenser > compressor > evaporator when  $\eta = 0.9$ . Further reordering takes place with EXV > condenser > evaporator with the compressor Irreversibility equal to zero when  $\eta = 1$  (isentropic compression). Identifying sources of systemic inefficiency is accomplished by examining the cycle through the agency of the Second Law. The heating coefficient of performance (COP) varies between  $4.10 \le COP_h$  2.22, while the cooling coefficient of performance varies from  $3.10 \le COP_c \le 4.22$ . These levels of performance and systemic inefficiencies in recent water heating and space

conditioning applications have also been documented for R410A [41, 38, 36]. These metrics, along with the absolute values of the thermal energy and work terms, are used to compare against the thermally-driven engine and heat pump system.

#### 4. Thermally-Driven Engine and Heat Pump

The thermally-driven engine consists of a distillation column with rectifying and stripping sections, an accumulator for refrigerant reflux, a solution heat exchanger between the absorber and the distillation column, and a solution pump. The heat pump, as in the case of the electrically-driven vapor compression case, consists of an evaporator, a condenser, and an EXV. The assumptions for the thermally-driven engine are (1) the reflux ratio is held constant at 0.50; (2) the solution pump efficiency  $(\eta_{pump})$  is taken as 0.85; (3) the ammonia concentration in the absorber is 95% of its equilibrium value; (4) the concentration of ammonia entering the absorber as a fraction of the concentration leaving the absorber is 0.5; and (5) there is equilibrium between the liquid and vapor phases in the evaporator and condenser. The temperature differential between the solution fed to the absorber is kept 5 bove the temperature of the solution leaving the absorber after heat is transferred from the absorber to a utility stream. These assumptions are practical and reasonable. The effect of higher and lower reflux ratios and ammonia purity from the distillation column are discussed later in the paper.

#### 4.1. First Law Analysis of the Thermally-Driven Heat Pump

A single-stage absorption cycle as shown in 5 is used for this evaluation. For this analysis we used EES to model a thermally-driven ammonia-water heat pump that provides 175.6 kW of cooling. The output with state points and state variables is shown in Figure 5. Since this system is primarily driven with thermal energy (except for parasitic electricity used by the solution pump and controller), the mechanical work produced by the thermally-driven engine to

Table 6: Performance metrics of the electrically-driven heat pump at various compressor efficiencies;  $T_c = 50 \frac{\circ C}{C}$ ;  $T_e = 0 \circ C$ ; and  $T_o = 25 \circ C$ 

	Source energy	$=rac{ \dot{W} }{0.33}$	(kW)	172	133.4	120.4
$\supset$	$COP_h rac{ \dot{Q}_c }{ \dot{W} }$			4.10	4.99	5.22
	$COP_c = \frac{\dot{Q}_e}{ \dot{W} }$			3.10	3.99	4.22
	Condenser load		(kW)	-232.42	-219.70	-215.40
	ncy Work Output Evaporator load Condenser load $COP_c = \frac{\dot{Q}_c}{ W } COP_h \frac{ \dot{Q}_c }{ W }$ Source energy		(kW)	175.7	175.7	175.7
	Work Output		(kW)	-56.76	-44.03	-39.73
	Compressor efficiency			$\eta = 0.7$	$\eta = 0.9$	$\eta = 1.0$

drive the heat pump is obtained by applying Equation (4). The steady-state energy balance for the cyclic process around the heat pump reduces to  $\sum \dot{W}_{cv}$  +  $\sum \dot{Q}_{cv} = 0$ . Since  $\sum \dot{Q}_{cv} = \dot{Q}_c + \dot{Q}_e = -281.1 \text{ kW} + 175.6 \text{ kW} = -105.5 \text{ kW}$ ,  $\sum \dot{W}_{cv}$  is +105.5 kW, which is the total work that must be done on the heat pump by the thermally-driven engine to enable the heat pump to meet its demand.

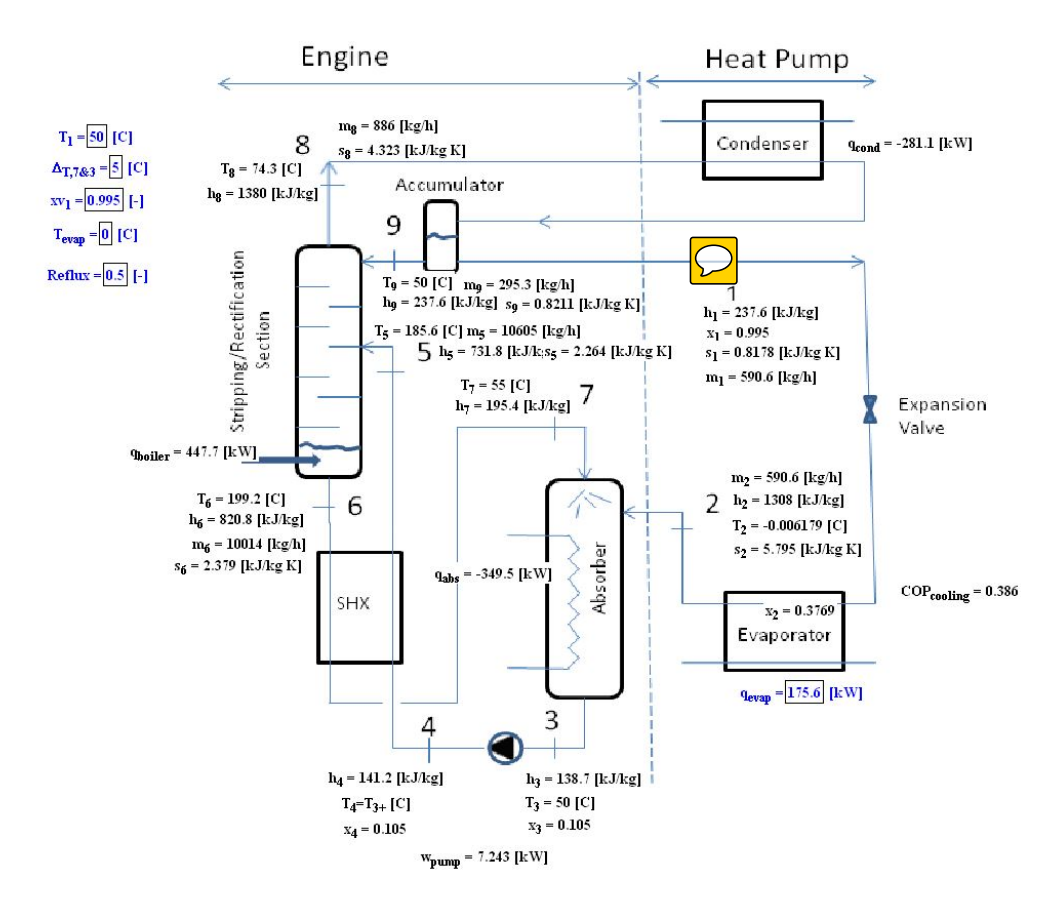


Figure 5: A single-stage ammonia-water absorption cycle demarcated into Engine and Heat Pump sections. The refrigeration load is fixed at 176.6 kW with  $T_e = 0$  °C;  $T_c = 50$  °C.

For a control volume encompassing the engine-heat pump configuration, the energy inflows and outflows summarized in Table 7 clearly show satisfaction of

Table 7: Energy balances around the absorption heat pump:  $T_c=50~^oC;~T_e=0~^oC;$  and  $T_o=25~^oC$ 

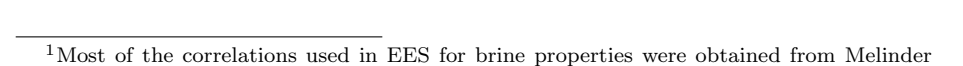
Component	Energy Input	Energy Output
	(kW)	(kW)
Evaporator	+175.6	
Condenser		-281.1
Absorber		-349.5
Pump	+7.24	
Boiler	+447.7	
Total	+630.54	-630.60



the overall energy balance within limits of acceptable computational accuracy.

#### 4.2. Second Law Analysis: Generic Non-Flow Configuration of the AHP

Similar to the case of the electrically-driven heat pump, a generic representation of the thermally-driven heat pump cycle of Figure 5 is shown in Figure 6, to which availability analysis is applied. This generic representation is independent of the nature of the refrigerant, fluid flow rates, or the engine type. For the same conditions, thermal loads, and temperatures as shown in Figure 5, the required minimum, actual work, and systemic Irreversibility distributed across the components is once again obtained by application of Equations (6)–(7). The results are tabulated in Table 8. Since the procedure is the same as the one applied to the generic electrically-driven heat pump shown in Figure 4, the details of the calculation are skipped for brevity. The algebraic sum of the evaporator and condenser availability is -105.7 kW, which must be supplied by the thermally-driven engine. The minimum work from the availability analysis (tabulated in Table 8, column three) is 37.85 kW. Since the total Irreversibility is 69.89 kW, the actual work supplied by the generic engine must be the sum of the minimum



(2010), reference [42]

work and the total Irreversibility, which equals 105.7 kW, and is in complete agreement with the previously calculated value from the First Law.

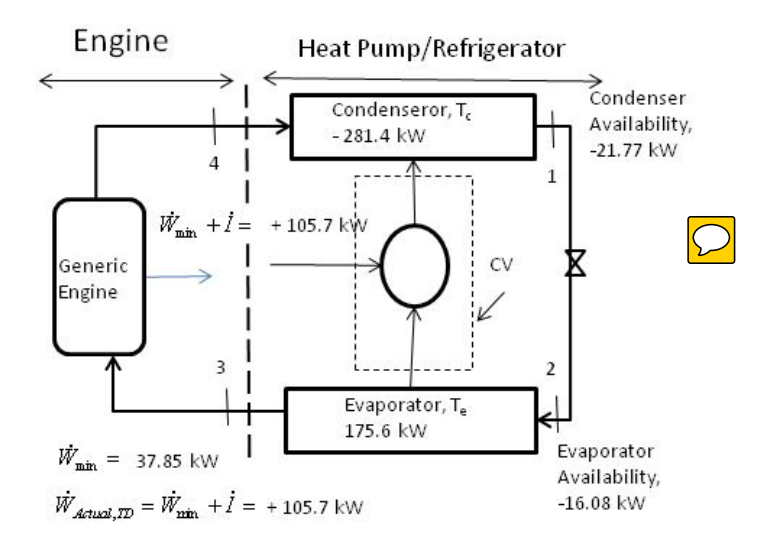


Figure 6: Minimum and actual work required by a thermally-driven engine to drive the generic heat pump operating between  $T_e = 0$  and  $T_c = 50$  °C, providing 175.6 kW of  $T_c = 0$  eration.

In order to further consolidate our availability analysis, we consider a heat pump providing the same 175.6 kW of refrigeration load except at an evaporator temperature of 5  $^{o}C$  instead of 0  $^{o}C$ , and rejecting the same 281.4 kW of heat to the condenser at 37.7  $^{o}C$  instead of 50  $^{o}C$ . Basically, the heat pump now provides a smaller temperature lift. Since the algebraic sum of the evaporator and condenser loads remains the same, the actual compressor work from an energy balance should also be the same, despite the smaller temperature lift from 37.7  $^{o}C$  to 50  $^{o}C$ . To prove the constancy of the actual work, we invoke availability analysis once again and summarize the results in Table 8. Due to the higher evaporator temperatures and lower condenser temperatures, their respective availabilities both drop. Since the temperature lift is lower, the minimum work is also lower at 24.13 kW. However, the total cycle Irreversibility increases to 81.61 kW, which when added to the minimum work of 24.13 kW equals 105.7 kW—as expected to satisfy the energy balance equation

[Equation (4)] as applied to the entire heat pump cycle.

# 4.3. Second Law Analysis: Flow Configuration of the Thermally-Driven Heat Pump

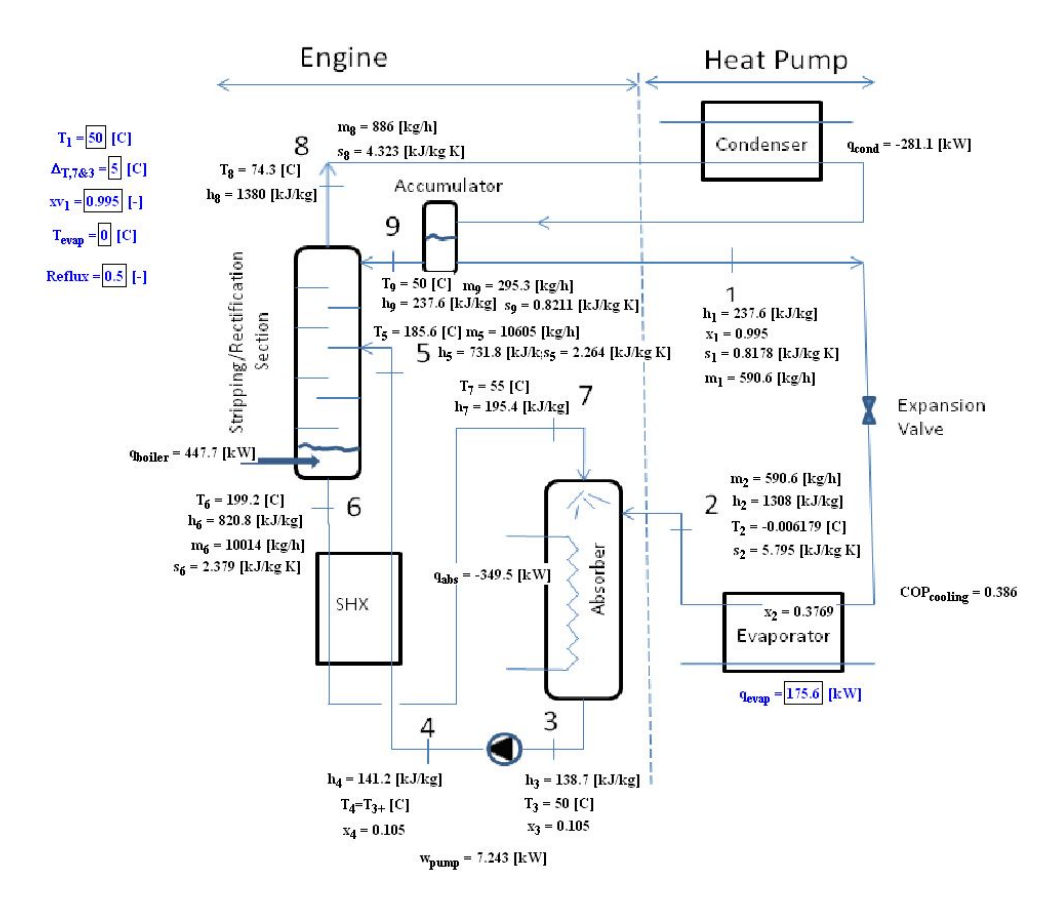


Figure 7: A single-stage absorption cycle demarcated into Engine and Heat Pump sections. The working pair is ammonia-water. The refrigeration load is fixed at 176.6 kW with  $T_e = 5$  °C;  $T_c = 37.7$  °C.

For a comprehensive analysis, we now use the Second Law for the flow process to calculate the work and Irreversibility for various components of the entire cycle. The state points used in the analysis are shown in Table 9. The data in this table comes from the EES model shown in Figure 5 for  $T_e = 0$  °C,  $T_c = 50$  °C,  $Q_{boiler} = +447.7kW$ ,  $Q_{abs}$  349.5kW, and  $Q_c = -281.1kW$ ;

Table 8: Minimum and actual work produced by the thermally-drivengine to drive the generic heat pump to provide 175.6 kW refrigeration at temperatures specified in the table

	$\dot{I} = T_o \dot{\sigma}$ $\dot{W}_{actual,TD} = \dot{W}_{min} + \dot{I}$	(kW)	105.7		$\dot{I} = T_o \dot{\sigma}$ $\dot{W}_{actual,TD} = \dot{W}_{min} + \dot{I}$	(kW)	1.05.7
		(kW)	62.89		$\dot{I} = T_o \dot{\sigma}$	(kW)	81.61
	$\dot{\sigma} = -\sum \left( \frac{Q_j}{T_j} \right)$	(kW)	(82) 0		$\dot{\sigma} = -\sum \left(\frac{Q_j}{T_j}\right)$	(kW)	0.274
00	$\sum \frac{\dot{Q}e}{Te}$	5		00	$\Sigma \frac{\dot{Q}e}{T_e}$	[	0 315
$T_e = 0$ $^{o}C$ ; $T_c = 50$ $^{o}C$	$\sum \frac{\dot{Q}c}{T_c}$	<u>[</u>	- 87g	$T_e = 5 {}^{o}C; T_c = 37.7 {}^{o}C$	$\sum \frac{\dot{Q}_c}{T_c}$	TATE OF THE PARTY	- (06.)
$T_e = 0 \ ^oC;$	$\dot{W}_{min} = -\sum_j \dot{Q} \left( 1 - \frac{T_o}{T_j} \right)$	(kW)	37.85	$T_e = 5^{-0}$	$A_{e} = \dot{Q}_{e} \left( 1 - \frac{T_{o}}{T_{e}} \right) \left[ A_{c} = \dot{Q}_{c} \left( 1 - \frac{T_{o}}{T_{c}} \right) \right] \dot{W}_{min} = - \sum_{j} \dot{Q} \left( 1 - \frac{T_{o}}{T_{j}} \right) \left[ \dot{W}_{min} + \dot{W}_{min} \right] = 0$	(kW)	24.13
	$\dot{A}_e = \dot{Q}_e \left( 1 - rac{T_o}{T_e}  ight) \hspace{0.2cm} \dot{A}_c = \dot{Q}_c \left( 1 - rac{T_o}{T_c}  ight)$	(kW)	-21.77		$\dot{A}_{c} = \dot{Q}_{c} \left( 1 - \frac{T_{o}}{T_{c}} \right)$	(kW)	-11.50
	$\dot{A}_e = \dot{Q}_e \left( 1 - \frac{To}{Te} \right)$	(kW)	-16.08		$\dot{A}_{e} = \dot{Q}_{e} \left( 1 - \frac{T_{o}}{T_{e}} \right)$	(kW)	-12.63

and for the case when  $T_e = 5$  °C,  $T_c = 37.7$  °C,  $Q_{boiler} = 5.6kW$ ,  $Q_{abs} = -304.9kW$ , and  $Q_c = -278.8kW$  for the same reflux ratio (0.5) and evaporator load ( $Q_e = 176.6kW$ ) as shown in Figure 7. Note that although the evaporator load was kept the same as in Figure 5 (176.6 kW), the condenser load computed in EES in the latter case came out to be -278.8 kW, slightly different from the -281.1 kW stipulated in the previous case. The work necessary to drive the heat pump in these two cases is calculated using the Second Law analysis for the flow system.

The application of Equation (3) to the data in Table 9 enables the calculation of the minimum and actual work produced by the thermally-driven engine to drive the heat pump. The values for the two cases tabulated in Table 10 show consistent agreement with the availability analysis data shown in Table 8, albeit with the adjustment of the condenser load for the case with  $T_e = 5$  °C;  $T_c = 37.7$  °C.

The performance metrics of the thermally-driven engine summarized in Table 11 display the amount of energy required by the boiler to meet the refrigeration load for the specified evaporator and condenser temperatures. The thermally-driven engine must convert thermal energy to the mechanical energy required to drive the heat pump. However, this conversion comes at the cost of discarding approximately two-thirds of the input energy out into the environment, similar to the conversion of thermal energy to electrical energy in a typical power plant. This discarded thermal energy has to express itself somewhere in the engine-heat pump cycle. Other than parasitic losses, the two places for energy rejection are the condenser and the absorber. A natural consequence of the thermally-driven engine producing the required mechanical work to drive a heat pump is the rejection of large amounts of heat through the condenser and the absorber. A second consequence is more cyclic Irreversibility due to thermal transfers, which must be overcome by the engine through producing the necessary extra work output. Characteristically, a major portion of the work produced by the thermally-driven engine is consumed to overcome cyclic inefficiencies. Substantial heat dissipation is an innate characteristic of thermally-

Table 9: State points from simulation in EES for the thermally-driven engine for two sets of evaporator and condenser conditions

Thermally-driven engine with heat pump operating between $T_e = C$ ; $T_c = 50$ °C;								
$Q_{boiler}$ =	= +447.7kW; Q	$_{abs} = -349$	$.5kW; Q_c =$	-281.1kW; reflux	ratio = $0.5$			
State Point	Temperature	Pressure	Enthalpy	Entropy	Mass flow rate			
	$(^{o}C)$	(bar)	$kJ \cdot kg^{-1}$	$kJ \cdot kg^{-1} \cdot K^{-1}$	$kg \cdot s^{-1}$			
1	50	20.26	237.6	0.8178	0.1641			
2	0	0.5018	1308	5.795	0.1641			
3	50	0.5018	138.7	2.9458				
4	50	20.26	141.2	2.9458				
5	185.6	20.26	731.8	2.9458	2.264			
6	199.2	20.26	820.8	2.7817	2.379			
7	55	0.5018	195.4	2.7817				
8	74.3	20.26	1380	0.2461	4.323			
9	50	20.26	237.6	0.0820	0.8211			
Thermally-d	riven engine wit	h heat pun	p operating	between $T_e = 5$ °c	$C; T_c = 37.7  {}^{o}C;$			
$Q_{boiler}$ =	= +405.6kW; Q	$_{abs} = -304$	$.9kW; Q_c =$	-278.8kW; reflux	ratio = 0.5			
1	37.7	14.51	175.9	0.0.6262	0.15389			
2	4.984	0.6923	1317	5.672	0.1539			
3	37.7	0.6923	27.38		1.40167			
4	37.7	14.51	29.15		1.40167			
5	146.9	14.51	521.2	1.886	1.40167			
6	170.1	14.51	665.4	2.11	1.24778			
7	42.7	0.6923	112.7		1.24778			
8	65.64	14.51	1384	4.473	0.23083			
9	37.7	14.51	175.9	0.6262	0.76944			

driven systems that must produce mechanical work to drive a connected cyclic system like a heat pump.

#### 4.4. Some Peculiarities of the Thermally-Driven Sorption Engine

Here we consider the effect of the reflux ratio and the evaporator temperature to illustrate some of the thermally-driven system's sensitivities in absorption systems as shown in the EES model. The main purpose of the reflux is to ensure that the output from the distillation column provides the proper level of ammonia purity for the solution that circulates in the heat pump portion of the cycle. Higher reflux ratios tend to favor higher ammonia purity going to the condenser. The increase in reflux ratio leads to an increase in the heat duty of the boiler as shown in Figure 8.

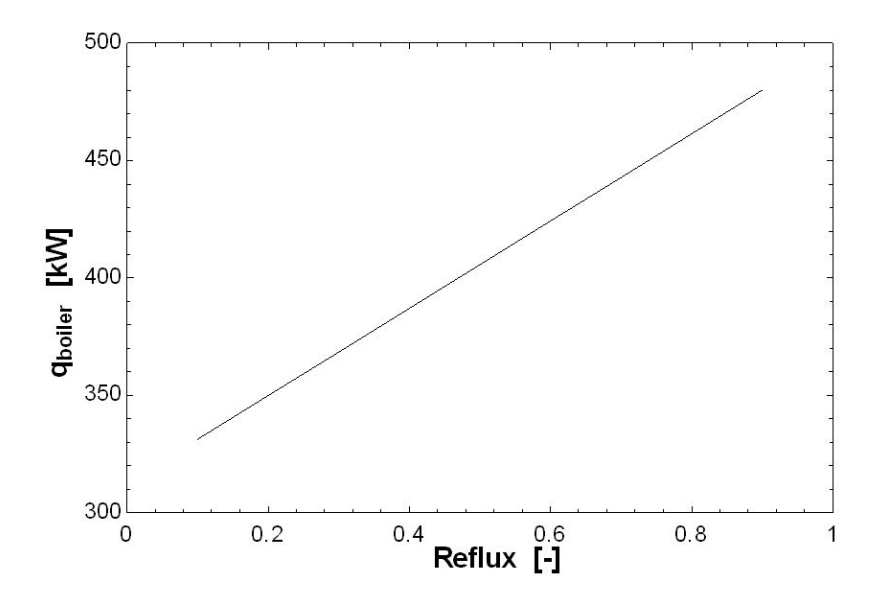


Figure 8: The effect of the reflux ratio on boiler heat input. The refrigeration load is fixed at 176.6 kW, with  $T_e = 5$   $^oC$ ;  $T_c = 37.7$   $^oC$ .

The effect of temperature lift on pump energy is significant. At the high temperature lift of 50  $^{o}C$ , the pump work is 7.24 kW; whereas at the lower lift of 32.7  $^{o}C$ , the pump work is 2.48 kW (Table 10) at a constant refrigeration load of 175.6 kW. This is because the solution mass flow rate is higher in the

Table 10: Minimum and actual work supplied by the thermally-driven engine to drive the heat pump

	$p^c \mid \dot{W}_{Engir}^a$	(kW)	-105.4		-103.2	
	$\dot{W}^r_{Engine} + \dot{W}_{pum}$	(kW)	-145.314		-123.166	
	$\dot{\sigma}_{abs,Engine} = -\sum_{j}rac{Q_{j}}{T_{j}}^{b} \; \left  \; \; \dot{W}_{Engine}^{r} + \dot{W}_{pump}^{\; c} \; \right $	$(kW \cdot K^{-1})$ 0.133727			0.067037	
	$\frac{\dot{Q}_{abs}}{T_{abs}}$	$(kW \cdot K^{-1})$	-1.081541		-9808589	
c gc	$\dot{W}_{pum}$ $\overrightarrow{\dot{Q}_{boiler}}$	(kW) $(kW \cdot K^{-1})$ $(kW \cdot K^{-1})$	-7.24 0.947814	2.7 °C	-52.319 $-2.48$ $0.913822$	
$T_e = 0$ $^{o}C; T_c$	Wpum	(kW)	-7.24	$V_e$ = 5 $^o$ $C$ ; $T_c$ = 37.7 $^o$ $C$	-2.48	F
$T_e =$	$\dot{W}_{min}{}^a$	(kW)	4	(Te) = 5	-52.319	
	$\dot{Q}_{abs} \left( 1 - \frac{T_o}{T_{abs}} \right)$	(kW)	-27.039		-12.457	E
	oiler $\left(1 - \frac{T_o}{T_{boiler}}\right)$	(kW)	164.109		133.144	;) ; = ;;
	Q					
	$\sum_{out} \dot{m} \left( h - T_o s \right) \; \left  \; \sum_{in} \dot{m} \left( h - T_o s \right) \; \right  \; \dot{Q}_{boiler} \left( 1 \right)$	(kW)	-69.459		-58.402	

 $^{a}W_{min} = \sum_{out} \dot{m} \left( h - T_o s \right) - \sum_{in} \dot{m} \left( h - T_o s \right) - \left( \dot{Q}_{boiler} \left( 1 - \frac{T_o}{T_{boiler}} \right) + \dot{Q}_{abs} \left( 1 - \frac{T_o}{T_{abs}} \right) \right)$   $^{b} \dot{\sigma}_{abs, Engine} = - \sum_{j} \frac{\dot{Q}_{j}}{T_{j}} = \frac{\dot{Q}_{boiler}}{T_{boiler}} + \frac{\dot{Q}_{abs}}{T_{abs}}$   $^{c} \dot{W}_{Engine}^{T} = \dot{Q}_{boiler} \left( 1 - \frac{T_o}{T_{boiler}} \right) + \dot{Q}_{abs} \left( 1 - \frac{T_o}{T_{abs}} \right) + \dot{W}_{pump}$ 

Table 11: Performance metrics of the thermally-driven heat pump;  $T_c = 50$  °C;  $T_e = 0$  °C; and  $T_o = 25$  °C

	Source energy <sup>a</sup>	$=\dot{Q}_{boiler}+\dot{W}_{pum}$	(kW)	447.7 + 21.95 = 469.65		405.6 + 7.512 = 413.1	
	$COP_h = \frac{\dot{Q}_c + \dot{Q}_{abs}}{\dot{Q}_{boiler} + \dot{W}_{pump}}$			1		<del>1</del> <del>1</del> <del>1</del> <del>3</del> 0	
$T_e = 0 \ ^oC; \   \{ \} \} \ 50 \ ^oC$	$\dot{V}_{pump}$			0.386	$C_{c} = 5  ^{o}C;  T_{c} = 37.7  ^{o}C$	0.430	1000 s
$T_e =$	Pump		(kW)	7.243		2.479	-
	Absorber		(kW) $(kW)$	-349.5 7.243		-304.9	<u> </u>
	Condenser		(kW)	-281.1		-278.8	-
	Work Output Evaporator Condenser		(kW)	175.6		175.6	
	Work Output		(kW)	-105.4		-103.2	

 $^a\mathrm{The}$  conversion of pump energy to source energy consumption is taken at a conversion efficiency of 33%.

former case than in the latter (Table 9). Therefore, pump selection over a wide range of flow rates is important for the thermally-driven engine.

The variation of ammonia purity entering the evaporator has a dramatic effect on performance, as illustrated for three typical values of evaporator pressure in Figure 9. As we move slightly away from pure ammonia, to about 99% ammonia purity, there is a drastic increase in the minimum evaporator temperature for the evaporator to work properly. This implies that the ambient temperature cannot go below the temperature corresponding to the specific purity and pressure. The plot highlights the severe limitation that ammonia purity imposes on evaporator operation and performance. A slight deviation from pure ammonia has a very large penalty on the ability of the evaporator to function. The net result is low cooling and heating COPs.

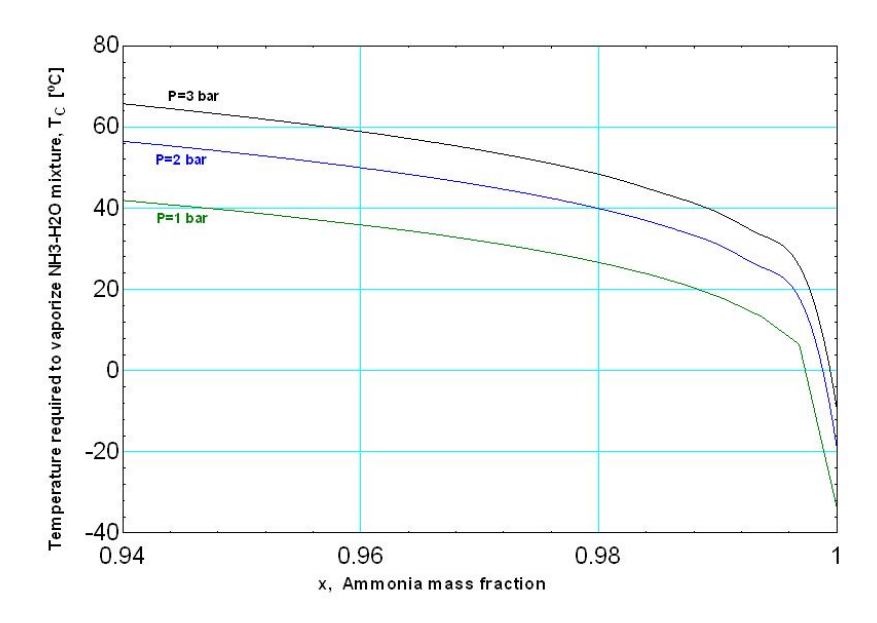


Figure 9: Limitations of evaporator temperature caused by varying ammonia purity.

#### 5. Discussion

This paper has highlighted and compared essential features of the electricallydriven and thermally-driven engines used to drive heat pumps for refrigeration and heating applications. The approach is comprehensive, invoking both First and Second Laws of thermodynamics to understand the nature of, and to quantify, the inherent "Lost Work" in both types of engines. We investigated the obvious question: Which of the two engines presents a better choice for driving a heat pump? In this quest, we exhaustively apply the Second Law of Thermodynamics to make our conclusions about the two engines.

The choice of an engine for driving the heat pump depends on whether the goal is to (1) provide refrigeration or thermal energy for a space or (2) provide water heating. We fix the refrigeration load between predetermined condenser and evaporator temperatures to provide a common basis for analysis. We show explicitly in Table 6 that a compressor with  $\eta = 0.7$  has a  $COP_c = 3.10$  and consumes 172 kW at the source. Higher compressor efficiencies have higher  $COP_c$ and consume even less energy at the source. In comparison, the thermallydriven heat pump providing the same refrigeration load, at the same condenser and evaporator temperatures, has a  $COP_c = 0.386$  and consumes 447.7 kW at the source. Since the burden of energy consumption, environmental pollution, and green hou has emissions is eventually traced to the source, the thermallydriven heat pump is most likely not a viable candidate for refrigeration unless there are copious amounts of solar energy or waste heat available at an acceptable temperature to drive the engine that would otherwise be discarded anyway. The electrically-driven engine fulfills its refrigerant load and discards far less energy in the condenser.

The basis for comparison is the same when considering a heating application (i.e., fixed refrigeration load, evaporator temperature, and condenser temperature). Table 6 indicates that for the electrically-driven heat pump the heating provided is -232.42 kW (through the condenser only) at a heating  $COP_h = 4.10$ , with a source energy consumption of 172 kW assuming that  $\eta = 0.7$ . The ratio of heating to source energy consumption is then 1.36 to 1. The thermally-driven heat pump, on the other hand, has a  $COP_h = 1.386$ , provides 630.6 kW (through the condenser and the absorber), while consuming 469.65 kW at source. The ratio of heat delivered to source energy consumption

is 1.34 to 1, no better than its competition.

A thermally-driven engine has additional operational burden to ensure that it can fulfill the power requirements to drive the heat pump. In the case of the absorption system, refrigerant purity, reflux ratio, and their impacts on pump power and evaporator performance are significant. A small deterioration in refrigerant purity can have a large adverse effect on the overall system performance. The electrically-driven engine and heat pump do not suffer from these problems. Overall, the electrically-driven engine is more compact and robust, whereas the thermally-driven system is prone to fluctuations which may significantly alter its performance.

Availability analysis on generic representations for both systems represented in Figures 4 and 6 yield the minimum, actual work, and systemic Irreversibilities, as tabulated in Tables 3 and 8. The total Irreversibility of the electrically-driven and thermally-driven heat pumps are 22.7 kW and 67.89 kW, respectively ( $\eta = 0.7$ ). The availability analysis is confirmed by considering the consistent values for work and Irreversibility for the steady-state flow configurations, as documented in Tables 4 and 10, respectively.

The conversion of heat to electricity in an electric power generation plant is about 33% efficient, with the remainder of heat discarded to the ambient air. The electricity generated to drive the compressor is high quality and should be used for refrigeration, not for producing heat. The reason is that if heat is used to generate electricity, and then if that electricity is used to generate heat, we are degrading a very useful form of energy (electricity) to a less useful form (heat), which is not a wise choice. This is an argument against using resistance heat as an example. On the other hand, if heating is the sole objective, then from the point of view of energy conservation and sustainability, the best heat source would be solar or some other thermal source that is discarded anyway as a by-product of a process. Heat pumps require mechanical work. If this work is produced by burning natural gas as in a thermally-driven engine, the conversion of heat to work must discard approximately two-thirds as waste heat. In a power plant this heat is discarded to the ambient air. In the case

of the thermally-driven engine it is expressed as heat discarded in the absorber and the condenser. That is why the thermal loads of the condenser and the absorber are so much higher for the same evaporator load as compared to the electrically-driven system. These observations are also reflected by Ziegler [12] in that the waste heat of an absorption chiller will always be larger than that of a compression chiller for a given cooling load. He goes on to say, "It can be expected that there are significant improvements in the efficiency of power plants and compression cooling systems: consequently we find that sorption technology must improve its performance considerably also in order to stay competitive" ([12]). The inherent higher Irreversibilities in the thermally-driven system is a thermodynamic fact. The net result is larger equipment sizes and a high dependence of these engines on environmental conditions to deliver the necessary power to drive heat pumps efficiently. In the specific case shown in Table 11, 469.65 kW is consumed at the source to provide 105.4 kW of useful work, representing a conversion efficiency of 22%, not as efficient as a modern power plant. Thermally-driven engines are not industrious converters of heat to mechanical work. They are an option when heat is freely or readily available or fuel switching is unfavorable.

#### 440 Acknowledgments

This work was supported by the U.S Department of Energy, Office of Energy Efficiency and Renewable Energy with A. Bouza as the Technical Program Manager. The authors are grateful to Prof. William Worek of Texas A & M University for reviewing the manuscript and offering helpful suggestions. Gratitude is expressed to Dr. Bo Shen, Dr. Brian Fricke, Dr. Kashif Nawaz, Ahmad Abu-Heiba, and Van Baxter for reviewing the manuscript. The Engineering Equation Solver (EES) software used is Professional V10097-3D. Spreadsheet calculations were made in Microsoft Excel 2010. The LaTeX editor used TeXstudio Qt Version 5.4.1.

#### 450 References

- J. Calm, "refrigerant transitions...again", moving towards sustainability, Proceedings of the ASHRAE/NIST Conference, Gaithersburg, MD, USA, 2012.10.29-30.
- [2] B. Palm, Hydrocarbons as refrigerants in small heat pump and refrigeration
   systems-a review, International Journal of Refrigeration 31 (4) (2008) 552–563.
  - [3] J. C. Bruno, A. Valero, A. Coronas, Performance analysis of combined microgas turbines and gas fired water/libr absorption chillers with postcombustion, Applied Thermal Engineering 25 (1) (2005) 87–99.
- [4] E. Torrella, D. Sánchez, R. Cabello, J. A. Larumbe, R. Llopis, On-site real-time evaluation of an air-conditioning direct-fired double-effect absorption chiller, Applied Energy 86 (6) (2009) 968–975.
  - [5] C. W. Park, J. Koo, Y. T. Kang, Performance analysis of ammonia absorption gax cycle for combined cooling and hot water supply modes, International Journal of Refrigeration 31 (4) (2008) 727–733.
  - [6] Y. T. Kang, H. Hong, K. S. Park, Performance analysis of advanced hybrid gax cycles: Hgax, International Journal of Refrigeration 27 (4) (2004) 442– 448.
- [7] M. Garrabrant, R. Stout, P. Glanville, J. Fitzgerald, C. Keinath, Development and validation of a gas-fired residential heat pump water heater-final report, Tech. rep., Stone Mountain Technologies, Inc. (2013).
  - [8] S. M. Tarique, M. A. Siddiqui, Performance and economic study of the combined absorption/compression heat pump, Energy Conversion and Management 40 (6) (1999) 575–591.
- [9] M. Kim, Y. J. Baik, S. R. Park, K. C. Chang, H. S. Ra, Design of a high temperature production heat pump system using geothermal water at moderate temperature, Current Applied Physics 10 (2) (2010) S117–S122.

- [10] L. F. Mendes, M. Collares-Pereira, F. Ziegler, Supply of cooling and heating with solar assisted absorption heat pumps: An energetic approach, International Journal of Refrigeration 21 (2) (1998) 116–125.
- [11] H.-M. Henning, Solar assisted air conditioning of buildings—an overview, Applied Thermal Engineering 27 (10) (2007) 1734–1749.
- [12] F. Ziegler, Recent developments and future prospects of sorption heat pump systems, International Journal of Thermal Sciences 38 (3) (1999) 191–208.
- [13] D. Lindenberger, T. Bruckner, H. M. Groscurth, R. Kümmel, Optimization of solar district heating systems: Seasonal storage, heat pumps, and cogeneration, Energy 25 (7) (2000) 591–608.
  - [14] A. Sözen, D. Altıparmak, H. Usta, Development and testing of a prototype of absorption heat pump system operated by solar energy, Applied Thermal Engineering 22 (16) (2002) 1847–1859.
  - [15] L. Fu, Y. Li, S. Zhang, Y. Jiang, A district heating system based on absorption heat exchange with chp systems, Frontiers in Energy 4 (1) (2010) 77. doi:10.1007/s11708-010-0022-0. URL http://journal.hep.com.cn/fie/EN/abstract/article\_9058. shtml
  - [16] F. Lin, T. Guansan, S. Jun, J. Yi, Combining absorption heat pump with gas boiler for exhaust condensing heat recovery in district heating system, Acta Energiae Solaris Sinica 24 (2003) 620–624.
- [17] K. J. Chua, S. K. Chou, W. M. Yang, Advances in heat pump systems: Areview, Applied Energy 87 (12) (2010) 3611–3624.
  - [18] K. E. NTsoukpoe, N. Le Pierrès, L. Luo, Experimentation of a libr-h2o absorption process for long term solar thermal storage, Energy Procedia 30 (2012) 331–341.

- [19] C. W. Chan, J. Ling-Chin, A. P. Roskilly, A review of chemical heat pumps, thermodynamic cycles, and thermal energy storage technologies for low grade heat utilisation, Applied Thermal Engineering 50 (1) (2013) 1257– 1273.
  - [20] W. Wu, B. Wang, W. Shi, X. Li, Absorption heating technologies: A review and perspective, Applied Energy 130 (2014) 51-71. doi:doi:10.1016/j.apenergy.2014.05.027.
    URL http://www.sciencedirect.com/science/article/pii/S0306261914005224
  - [21] K. Abrahamsson, S. Stenström, G. Aly, Å. Jernqvist, Application of heat pump systems for energy conservation in paper drying, International Journal of Energy Research 21 (7) (1997) 631–642.
  - [22] B. Le Lostec, N. Galanis, J. Baribeault, J. Millette, Wood chip drying with an absorption heat pump, Energy 33 (3) (2008) 500–512.
  - [23] Y. Wang, N. Lior, Thermoeconomic analysis of a low-temperature multieffect thermal desalination system coupled with an absorption heat pump, Energy 36 (6) (2011) 3878–3887.
  - [24] X. Zhang, D. Hu, Z. Li, Performance analysis on a new multi-effect distillation combined with an open absorption heat transformer driven by waste heat, Applied Thermal Engineering 62 (1) (2014) 239–244.
- [25] R. Gomri, Thermal seawater desalination: Possibilities of using single effect
   and double effect absorption heat transformer systems, Desalination 253 (1)
   (2010) 112–118.
  - [26] Y. Ammar, H. Li, C. Walsh, P. Thornley, V. Sharifi, A. P. Roskilly, Desalination using low grade heat in the process industry: Challenges and perspectives, Applied Thermal Engineering 48 (2012) 446–457.

- [27] A. Gidner, Å. Jernqvist, G. Aly, An energy efficient evaporation process for treating bleach plant effluents, Applied Thermal Engineering 16 (1) (1996) 33–42.
  - [28] M. Scott, Å. Jernqvist, J. Olsson, G. Aly, Experimental and theoretical study of an open multi-compartment absorption heat transformer for different steam temperatures. part i: Hydrodynamic and heat transfer characteristics, Applied Thermal Engineering 19 (3) (1999) 279–298.
  - [29] J. Kirkland, Natural gas could serve as "bridge" fuel to low-carbon future, Scientific American 1.

URL http://www.scientificamerican.com/article/
natural-gas-could-serve-as-bridge-fuel-to-low-carbon-future/

- [30] White House, FACT SHEET: U.S. Reports its 2025 Emissions Target to the UNFCCC (2015).
  URL http://www.whitehouse.gov/the-press-office/2015/03/31/
  - fact-sheet-us-reports-its-2025-emissions-target-unfccc
- [31] NASA, Carbon Dioxide: Latest Measurements, June 2016 (2016).

  URL http://climate.nasa.gov/vital-signs/carbon-dioxide/
  - [32] D. Biello, Geophysicists Urge Steep Cuts in Greenhuse Gas Emissions, Scientific American.

URL http://www.scientificamerican.com/article/
geophysicists-urge-steep-cuts-in-greenhouse-gases/

- [33] K. Warke, Jr., Advanced Thermodynamics for Engineers, McGraw-Hill, New York; ISBN 0-07-068292-5, 1995.
- [34] V. Gold, K. L. Loening, A. D. McNaught, P. Shemi, Lupac compendium of chemical terminology, Blackwell Science, Oxford.
- [35] S. A. Klein, F. Alvarado, EES: Engineering equation solver for the Microsoft Windows operating system, F-Chart software, 1992.

- [36] M. R. Ally, J. D. Munk, V. D. Baxter, A. C. Gehl, Data, exergy, and energy analyses of a vertical-bore, ground-source heat pump for domestic water heating under simulated occupancy conditions, Applied Thermal Engineering 89 (2015) 192–203.
- [37] M. R. Ally, J. D. Munk, V. D. Baxter, A. C. Gehl, Exergy analysis of a two-stage ground source heat pump with a vertical bore for residential space conditioning under simulated occupancy, Applied Energy 155 (2015) 502–514.
- [38] M. R. Ally, J. D. Munk, V. D. Baxter, A. C. Gehl, Exergy analysis and operational efficiency of a horizontal ground-source heat pump system operated in a low-energy test house under simulated occupancy conditions, International Journal of Refrigeration 35 (4) (2012) 1092–1103.
- [39] M. A. Kedzierski, J. S. Brown, J. Koo, Performance ranking of refrigerants with low global warming potential, Science and Technology for the Built Environment 21 (2) (2015) 207–219.
  - [40] EIA, U.S. Energy Information Administration: What is the efficiency of different types of power plants? (2016). URL https://www.eia.gov/tools/faqs/faq.cfm?id=107&t=3
- [41] V. D. Baxter, R. W. Murphy, K. Rice, R. L. Linkous, High efficiency water heating technology development final report: Part i, lab/field performance evaluation and accelerated life testing of a hybrid electric heat pump water heater (hpwh), Tech. rep., Oak Ridge National Laboratory (ORNL), Oak Ridge, TN (United States). Building Technologies Research and Integration
   Center (BTRIC) (2016).
  - [42] Å. Melinder, Properties of Secondary Work Fluids\*/for Indirect Systems:\*/Secondary Refrigerants Or Coolants, Heat Transfer Fluids, International institute of refrigeration, 2010.